

Microstructure Evolution and Mechanical Properties of a Directionally Solidified NiAl-Mo Hyper-Eutectic Alloy

Zhang Jianfei, Xu Pengfei, Dong Yuelei, Hao Wenwei, Zhang Yuhao

Inner Mongolia University of Science and Technology, Baotou 014010, China

Abstract: A hyper-eutectic alloy, with nominal composition Ni-42Al-16Mo (at%), was directionally solidified at growth rates ranging in 12~300 $\mu\text{m/s}$ by liquid metal cooling (LMC) technique. Microstructural examination reveals that the NiAl-16Mo alloy is composed of primary Mo dendrite and NiAl/Mo eutectic cell in all the growth conditions employed. With the growth rates increasing from 12 to 300 $\mu\text{m/s}$, the volume fraction of Mo primary dendrite increases from 7.21% to 11.42%, while the size and the arm spacing of Mo primary dendrite reduces simultaneously. The corresponding room temperature fracture toughness (RTFT) and ultimate high temperature compressive strength (UTCS) decrease with the increase of growth rates. The toughening and strengthening mechanism of composite was also discussed.

Key words: crystal growth; intermetallics; fracture toughness; compressive strength

NiAl intermetallic compound offers desirable properties for high temperature structural applications compared with Nickel-based superalloys. There has been considerable interest in NiAl as a candidate material for high-temperature applications in aerospace vehicles due to its high melting point, superior oxidation resistance, good thermal conductivity, low brittle-to-ductile transformation-temperature (BDTT)^[1]. However, NiAl is brittle at room temperature (RT) and has poor strength at high temperature. To make NiAl a viable high temperature structural material, systematic efforts have been made to overcome its disadvantages through various fabrication processes^[2-6]. The directional solidification (DS) of eutectic alloys can effectively improve RTFT of intrinsically brittle NiAl intermetallics. According to the studies of Bei et al^[7] and Ferrandini et al^[8], NiAl-Mo alloy can generate a composite structure and improve the both properties. However, previous studies were all done at the eutectic composition (NiAl-9Mo, at%). It is well known that the properties of composites are greatly dependent on the microstructure and the volume fraction of the constituent phases. However the composition and process parameters influence the microstructures. Up to now,

the hyper-eutectic alloy of NiAl-Mo system is rarely studied. In the present investigation, the Ni-42Al-16Mo (at%) hyper-eutectic alloy was directionally solidified by LMC technology. The microstructure evolution, RTFT and UTCS of the alloy were investigated.

1 Experiment

The ingot ($\Phi 80$ mm \times 100 mm) with composition of Ni-42Al-16Mo (NiAl-16Mo in brief) was cast by a vacuum induction melting furnace under an argon atmosphere using a stainless steel die. The $\Phi 8.9$ mm \times 100 mm rods were cut from the ingot by Wire Electro-discharge Machine (EDM) and directionally solidified at 12~300 $\mu\text{m/s}$. The details of DS experiment are given in Ref[9]. We sectioned the DSed rods by EDM for metallographic analysis. After a series of metallographic processes, the specimens were etched by a solution of 80%HCl-20%HNO₃. The microstructures and composition were observed by a scanning electron microscope (SEM) equipped with energy dispersive spectrometry (EDS). The quantitative analysis was conducted by SISCIV8.0 metallurgical analysis software.

The compression specimens ($\Phi 4$ mm \times 10 mm) and

Received date: November 19, 2018

Foundation item: National Natural Science Foundation of China (51564041); the Natural Science Foundation of Inner Mongolia of China (2018MS05028); the Inner Mongolia University of Science and Technology Industry-Study-Research Found (PY201509)

Corresponding author: Zhang Jianfei, Ph. D., Associate Professor, College of Materials and Metallurgy, Inner Mongolia University of Science and Technology, Baotou 014010, P. R. China, Tel: 0086-472-5951572, E-mail: zhangjianfei_vip@163.com

Copyright © 2019, Northwest Institute for Nonferrous Metal Research. Published by Science Press. All rights reserved.

three-point bending (3PB) specimens were machined by EDM from the DSed samples along the growth direction. A schematic illustration of the fracture toughness composite specimen is shown in Fig.1.

The details of 3PB test are given in Ref[10]. The compression experiments were conducted with a Gleeble 1500D test machine at 1273 K at an initial strain rate of $2 \times 10^{-3} \text{ s}^{-1}$ and the compression axis was parallel to the growth direction. In this work, three or four specimens were tested and the average value was adopted for each specimen condition.

2 Results and Discussion

2.1 Microstructure

The solid-liquid (S/L) interface morphologies and transverse section microstructures of the directionally solidified NiAl-16Mo alloy at 12, 300 $\mu\text{m/s}$ and $G_L=334 \text{ K/cm}$ are shown in Fig.2 (for conciseness, selective metallographic images are presented). Fig.2a₁ and 2b₁ show the longitudinal section microstructures of the DSed alloy while Fig.2a₂ and 2b₂ display the transverse microstructures. Because of the hyper-eutectic composition, for all employed growth conditions, it is found that the alloy structure is composed of primary Mo dendrite phase and NiAl/Mo eutectic cell. The longitudinal microstructures present that both NiAl/Mo eutectics and primary Mo phase are aligned erectly along the growth direction and interfaces are characterized by the Mo dendrites prior to the eutectics. The cross microstructures show NiAl/Mo eutec-

tic cells, and that the fibrous Mo is distributed in the NiAl matrix. There are two changes with the increase of growth rate from 12 to 300 $\mu\text{m/s}$. First, the primary Mo dendrite arm spacing reduces. Second, the volume fraction of constituent phases varied. For example, the volume fraction of eutectics decreases from 92.79% to 88.58%. At the same time, the primary Mo dendrite arm spacing reduces from 230.80 to 127.10 μm (as is seen in Table 1). In our study, the primary Mo dendritic phases precipitate in the DSed alloy which shows that the alloy composition is outside the coupled growth zone. According to the theory of constitutional undercooling^[11]:

$$G_L / V \geq M_L (C_E - C_0) / D_L \quad (1)$$

where G_L is the temperature gradient in the liquid ahead of the interface, V is the growth rate, m_L is the liquids slope, M_L is the slope of the liquidus, D_L is the diffusion coefficient of solute atom in the liquid, C_E is the eutectic compo-

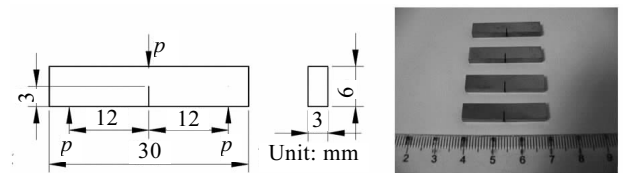


Fig.1 Schematic diagram of 3PB specimen

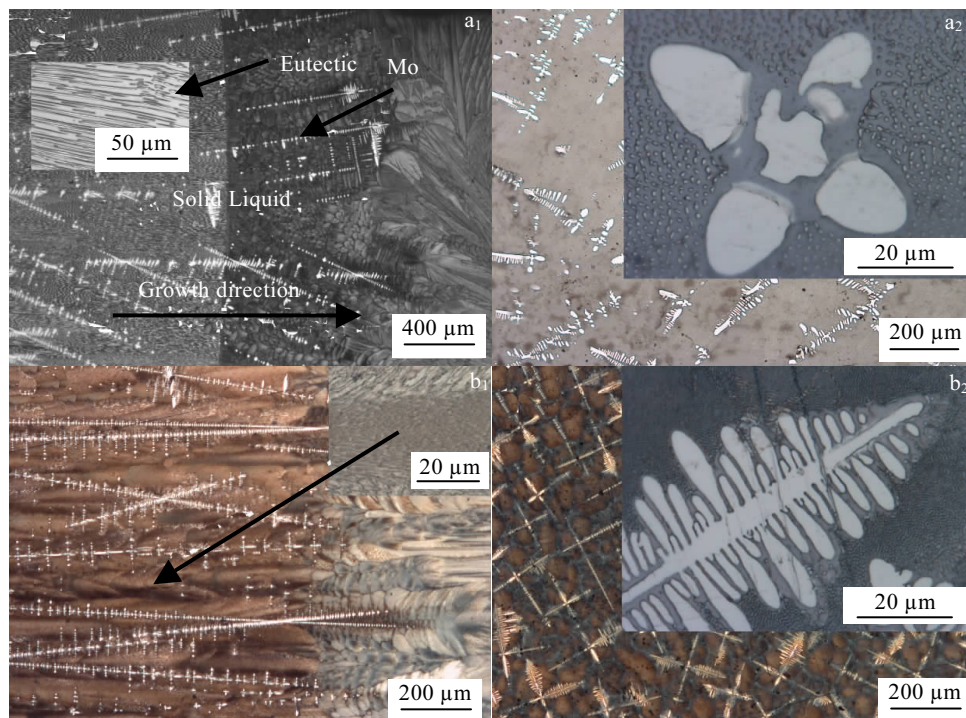


Fig.2 Optical metallographic images of quenched S/L interfaces and microstructures of DSed NiAl-16Mo alloy at 12 $\mu\text{m/s}$ (a₁, a₂); and 300 $\mu\text{m/s}$ (b₁, b₂): (a₁, b₁) longitudinal section; (a₂, b₂) transverse section

Table 1 Volume fraction of phases and the primary Mo dendrite spacing of DSed NiAl-16Mo alloy

Growth rate, $V/\mu\text{m}\cdot\text{s}^{-1}$	Primary Mo/ %	Eutectic/ %	Primary Mo dendrite spacing, $\lambda_1/\mu\text{m}$
12	7.21	92.79	230.80±45.30
25	7.89	92.11	199.13±39.85
50	8.65	91.35	171.90±39.40
100	9.58	90.42	166.05±43.05
300	11.42	88.58	127.10±26.95

sition, and C_0 is the initial composition of the solidifying alloy. The Eq.(1) shows that for a given composition the right side of Eq.(1) is a constant. It indicates that a large temperature gradient G_L and a small growth rate V should contribute to formation of regular in-situ composites with perceptible deviation of their nominal composition C_0 from the eutectic composition C_E . When Eq.(1) holds true, the interface is planar and the fully eutectic microstructure is obtained. When the value of G_L/V is low enough, it makes Eq.(1) indefensible. For the eutectic alloy, instability of two phases occur and the interface evolves from planar into cellular. For the off-eutectic alloy, single-phase instability happens and causes the mixed structures characterized by dendrites of one phase and interdendritic two-phase eutectic. Our group has observed a fully fibrous microstructure was in DSed NiAl-16Mo ($V=6\ \mu\text{m/s}$, $G_L=334\ \text{K/cm}$)^[10].

However, the occurrence of primary Mo dendrites in our study presents that the supercooling composition point under our experimental conditions ($V=12\sim 300\ \mu\text{m/s}$, $G_L=334\ \text{K/cm}$) is outside the coupled-growth zone. So the microstructure at RT is made up of primary αMo dendrite and ($\alpha\text{Mo}+\beta\text{NiAl}$) eutectic. It is also worth mentioning that the eutectic structure becomes irregular with the increase of the growth rate. For example, the Mo fibers are uniformly aligned along the growth direction at $V=12\ \mu\text{m/s}$, while at $V=300\ \mu\text{m/s}$, eutectic colony structures and the coarse regions at colony boundaries appear in the area of inter-dendritic. This will undoubtedly affect the properties of the alloy and will be discussed later.

The composition of NiAl matrix, eutectic and primary αMo dendrite were analyzed by EDS. Here we chose the specimen of $V=12\ \mu\text{m/s}$ to analyze the composition of the phases. The results show that the αMo dendrite contained all three elements and had the composition Mo-2.99Ni-8.64Al (at%), while the eutectic contains all three elements and has the composition Ni-44.69Al-10.37Mo (at%). And the NiAl matrix has the near-stoichiometric composition Ni-49.58Al (at%).

2.2 Fracture toughness

Table 2 shows the results of 3PB bending test and Fig.3 shows the representative applied stress-strain curve (all the curves are similar in the bending test, and here we choose the curve of $V=12\ \mu\text{m/s}$ to explain the phenomenon). It can be seen that the RTFT of all DSed NiAl-16Mo alloy is higher than that of NiAl ($5.15\ \text{MPa}\cdot\text{m}^{1/2}$ for comparison, the

RTFT of NiAl was tested in our study). From the curve we can conclude that the specimen fractures abruptly rather than fractures gradually from crack propagation. The failure mode is typical of brittle manner. A trend is noticed that the RTFT falls with the increase of growth rate in DSed NiAl-16Mo alloy. RTFT for the DSed NiAl-16Mo composites decreases gradually from $9.69\ \text{MPa}\cdot\text{m}^{1/2}$ to about $8.13\ \text{MPa}\cdot\text{m}^{1/2}$ with the increase of growth rate from $12\ \mu\text{m/s}$ to $300\ \mu\text{m/s}$. The RTFT of the DSed alloy varies greatly in the microstructural evolution because of the following three reasons: first, the volume fraction of eutectic NiAl/Mo in DSed alloy decreases with the increase of growth rate. The Mo fibers are the major toughening phases by crack bridging, crack trapping, crack blunting and crack linkage mechanism^[12]. Second, DS process refines the primary Mo dendrite and changes the morphology of eutectic around the dendrite, which has a harmful effect on the properties because the regularity of Mo fibers is essential to RTFT^[13]. Third, the decrease of dendrite spacing makes it easy to crack propagation along the Mo dendrite/NiAl matrix interface.

The fracture surface of the 3PB specimens for DSed NiAl-16Mo alloy was observed by SEM and shown in Fig.4. In all cases, the main crack in the DSed specimen initiates from the notch and propagates straightly, and is slightly tilted to the loading direction (Fig.4a). The side surface observation (Fig.4a) shows the Mo fibers are oriented perpendicular to the crack path. Plastic stretching of the Mo fibers is evident from inspection of the side surface (Fig.4b). The Mo fibers toughen the NiAl matrix through crack

Table 2 RTFT (K_Q) and UTCS ($1273\ \text{K}$, $2\times 10^{-3}\ \text{s}^{-1}$) of the present alloy at different growth rates

	Growth rate of DSed NiAl-16Mo/ $\mu\text{m}\cdot\text{s}^{-1}$					NiAl
	12	25	50	100	300	
$K_Q/\text{MPa}\cdot\text{m}^{1/2}$	9.69	9.18	9.34	8.76	8.13	5.15
UTCS/MPa	250.61	203.75	201.08	203.14	198.50	88.61

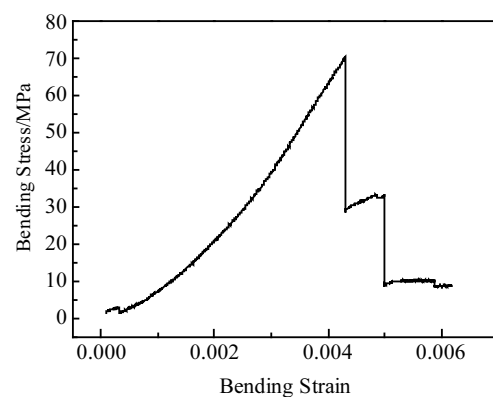


Fig.3 Stress-strain curve of DSed NiAl-16Mo alloy 3PB bending test ($V=12\ \mu\text{m/s}$)

bridging, crack trapping and crack linkaging. The regularity and the volume fraction of the Mo fibers are essential to the RT fracture toughness^[12]. As seen in Fig.4b, well-aligned Mo fibers inter-dendritic embed within NiAl matrix at $V=12 \mu\text{m/s}$. According to Table 2 and Fig.2, the volume fraction of eutectic structure decreases with the increase of growth rates, the regularity of Mo fibers around the Mo dendrites becomes worse, which is accompanied by the growth rates. Undoubtedly, these factors will weaken the toughening effect. Fig.4c reveals that the interface of Mo dendrite/NiAl matrix is the fracture initiation. It is shown that the primary NiAl is deformed first. A shallow dimple is left by primary Mo pulling out in the alloy (Fig.4d). This shows that the interface between Mo dendrite and NiAl matrix is weak. And this can facilitate the propagation of crack. Fractured Mo dendrite is also left in the matrix (Fig.4d). According to Table 1, the decrease in the primary Mo dendrite arm spacing makes it easy to extend the crack. All RTFT values here are lower than that of the fully fibrous specimen of DSed NiAl-16Mo alloy ($V=6 \mu\text{m/s}$, $K_Q=19.36 \text{ MPa}\cdot\text{m}^{1/2}$)^[10]. This indicates that the precipitation of the primary Mo phase affects the properties of the alloy.

2.3 High temperature compressive properties

Table 2 shows the results of compressive test and Fig.5 shows the compressive true stress-strain curves at 1273 K. For comparison, the strength of binary NiAl was also examined. The samples were compressed to about 50% engi-

neering strain. All curves are similar in appearance. With the increase of strain the true stress-strain curves reach rapidly a peak stress where strain softening occurs and then the stress decreases gradually. The UTCS of $V=12 \mu\text{m/s}$ possesses the highest value. For the growth rates ranging from 12~300 $\mu\text{m/s}$, the UTCS continuously decreases from 250.61 to 198.50 MPa. Just as seen in the values summarized in Table 2. The compressive strength of polycrystal NiAl at 1273 K is about 88.61 MPa. It can be concluded that DSed NiAl-16Mo alloy possesses better high temperature strength than polycrystal NiAl.

In the present work, the microstructure evolution is the major factor leading to the reduction of the UTCS with the growth rate. Firstly, the properties are compromised by the decrease in volume fraction of eutectic microstructure caused by increase of growth rates. Secondly, the eutectic cell boundaries which are weak at 1273 K counteracts the above strengthening mechanism. The boundaries of these cells are a discontinuity in the structure and the main crack always appears at the disturbed zone^[14]. With the increase of the growth rate, the total area of cell boundary increases gradually. In addition, the eutectic structure becomes irregular with the increasing of growth rate, and the regularity of the eutectic structure is essential for the properties of in-situ composite. These three factors can explain the phenomenon.

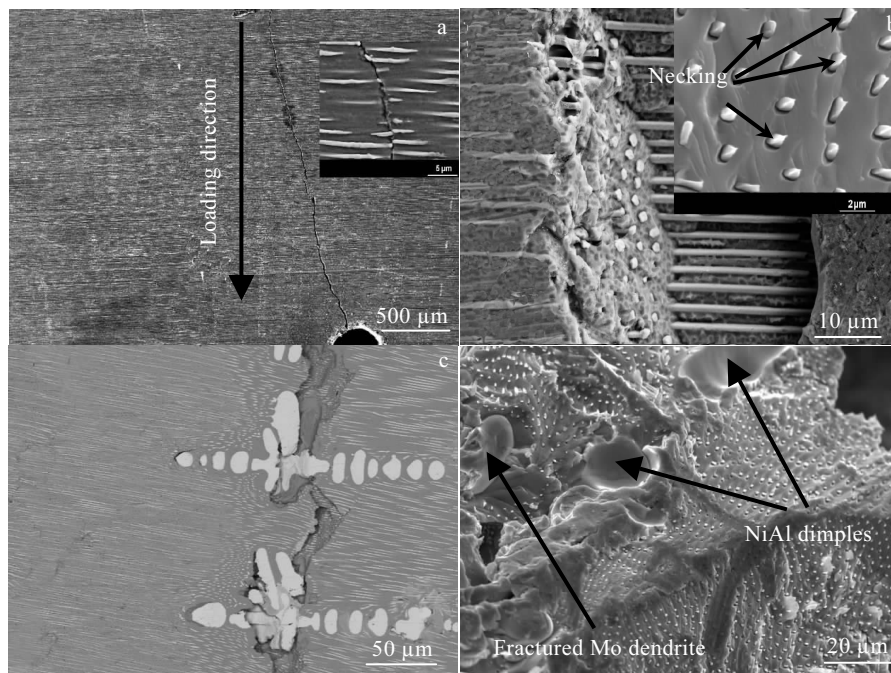


Fig.4 SEM images of fracture surface of materials after 3PB bending test at room temperature: (a) the path of cracks; (b) plastic stretching of the Mo fibers; (c) the fractured interface of Mo dendrite/NiAl matrix; (d) NiAl dimples and fractured Mo dendrite

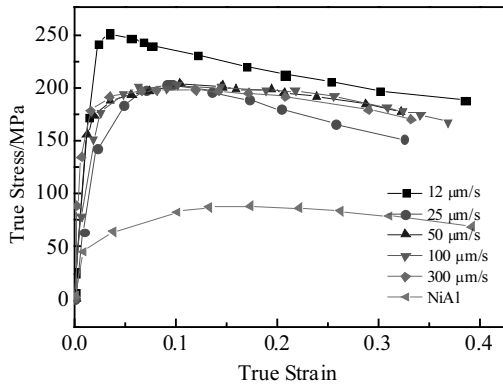


Fig.5 Compressive true stress-strain curves of alloys at 1273 K

3 Conclusions

1) Dependence of the microstructure evolution on the growth rates for the NiAl-16Mo alloys was studied. The supercooling composition point under our growth conditions ($V=12\sim 300\ \mu\text{m/s}$, $G_L=334\ \text{K/cm}$) is outside the coupled-growth zone. The microstructure of DSed NiAl-16Mo alloy is composed of primary Mo dendrite and eutectic ($\alpha\text{Mo}+\beta\text{NiAl}$).

2) The volume fraction of constituent phases can be changed accompanied with the growth rate. Simultaneously, the primary Mo dendrite arm spacing becomes fine.

3) The precipitation of the primary Mo phase and the microstructure evolution deteriorate the properties of the alloy. This phenomenon could be explained by two decisive factors. The one is that the volume fraction of eutectics de-

creases accompanied with the growth rate; the other is that the decrease in primary Mo dendrite arm spacing caused by increase of growth rates compromises the improvement of the properties.

References

- Guo J T, Xie Y, Sheng L Y et al. *Intermetallics*[J], 2011,19: 206
- Wang L, Shen J. *J Alloy Compd*[J], 2016, 663: 187
- Wang L, Shen J, Zhang Y P et al. *Intermetallics*[J], 2017, 84: 11
- Dong H X, Jiang Y, He Y H et al. *J Alloy Compd*[J], 2009, 484: 907
- Jiang D T, Guo J T. *Mater Lett*[J], 1998, 36: 33
- Xu K, Arsenault R J. *Acta Mater*[J], 1999, 47: 3023
- Bei H, George E P. *Acta Mater*[J], 2005, 53: 69
- Ferrandini P, Batista W W, Caram R. *J Alloy Compd*[J], 2004, 381: 91
- Zhang J F, Shen J, Shang Z et al. *Mater Charact*[J], 2015, 99: 160
- Zhang J F, Shen J, Shang Z et al. *Intermetallics*[J], 2012, 21: 18
- Kurz W, Fisher D J. *Fundamentals of Solidification*[M]. Switzerland: Trans Tech Publication Ltd, 1998: 54
- Joslin S M, Chen X F, Oliver B F et al. *Mater Sci Eng A*[J], 1995, 196: 9
- Seemuller C, Heilmaier M, Haenschke T et al. *Intermetallics*[J], 2013, 35: 110
- Hu L, Hu W, Gottstein G et al. *Mater Sci Eng A*[J], 2012, 539: 211

定向凝固 NiAl-Mo 过共晶合金组织演变及性能

张建飞, 徐鹏飞, 董悦雷, 郝文纬, 张宇昊

(内蒙古科技大学, 内蒙古 包头 014010)

摘要: 采用液态金属高温梯度定向凝固装置制备了 NiAl-16Mo (原子分数, %) 过共晶合金, 研究了生长速率对合金组织演变及性能的影响。结果表明: 在生长速率为 $12\sim 300\ \mu\text{m/s}$ 范围内, 该合金的凝固组织为初生 Mo 枝晶与 NiAl/Mo 纤维共晶的混合组织。随生长速率的增加, 初生 Mo 枝晶的体积分数由 $12\ \mu\text{m/s}$ 的 7.21% 增加到 $300\ \mu\text{m/s}$ 的 11.42%, Mo 枝晶尺度和间距同时随之减小。力学性能测试结果表明, 室温断裂韧性和高温强度随生长速率增加而降低, 同时对合金强化机理进行了探讨。

关键词: 晶体生长; 金属间化合物; 断裂韧性; 压缩强度

作者简介: 张建飞, 男, 1976 年生, 博士, 副教授, 内蒙古科技大学材料与冶金学院, 内蒙古 包头 014010, 电话: 0472-5951572, E-mail: zhangjianfei_vip@163.com